Modeling Motion Blur in Computer-Generated Images

Michael Potmesil[1]
Bell Laboratories

Indranil Chakravarty[2]
Schlumberger-Doll Research

Abstract

This paper describes a procedure for modeling motion blur in computer-generated images. Motion blur in photography or cinematography is caused by the motion of objects during the finite exposure time the camera shutter remains open to record the image on film. In computer graphics, the simulation of motion blur is useful both in animated sequences where the blurring tends to remove temporal aliasing effects and in static images where it portrays the illusion of speed or movement among the objects in the scene.

The camera model developed for simulating motion blur is described in terms of a generalized image-formation equation. This equation describes the relationship between the object and corresponding image points in terms of the optical system-transfer function. The use of the optical system-transfer function simplifies the description of time-dependent variations of object motion that may occur during the exposure time of a camera. This approach allows us to characterize the motion of objects by a set of system-transfer functions which are derived from the path and velocity of objects in the scene and the exposure time of a camera.

CR Categories and Subject Descriptors: **I.3.7 [Computer Graphics]:** Three-Dimensional Graphics and Realism, **I.4.4 [Image Processing]:** Restoration

General Terms: Algorithms

Key Words and Phrases: Camera Model, Motion Blur, Point-Spread Function, Image Restoration, Digital Optics

1.0 Introduction

The generation of computer-synthesized images with a high degree of realism has been the topic of much current research. The increase in realism in recent years can be attributed mainly to improved shading techniques and to more versatile 3D object modeling techniques that can represent complex objects with great detail. The objective of this paper is to report an image synthesis technique which incorporates the optical effects of a camera in imaging a scene. These optical effects of a camera add another dimension of realism in computer generated images. In this paper we attempt to model *motion blur*, an effect caused by the movement of objects during the exposure time of the camera, and used often to portray to the viewer the illusion of the motion of objects.

In a previous paper [6,7] the authors developed a technique for modeling the effects of a lens and aperture in a camera model for computer-synthesized images. This paper is both an extension and a generalization of the previous paper to incorporate the effects of the camera shutter. In addition, this paper presents the image-generation process in terms of a cascaded optical, system-transfer function which specifies the relationship between object and image points. This formalism allows us to express easily the time-dependent variations of an object's position and provides a more comprehensive approach to synthesizing the effects of motion blur and other camera effects.

The appearance of motion blur in images can occur due to a number of reasons. The primary cause of this blurring is due to the movement of an object's position in the scene during the exposure time of the camera. By *exposure time* we mean the time during which the camera shutter remains open and the film acts as an integrating medium to accumulate the total radiant energy of the objects in the scene. There are two principal reasons for motion blur:

1. Address: Bell Laboratories, Holmdel, NJ 07733
2. Address: Schlumberger-Doll Research Center, Old Quarry Road, Ridgefield, CT 06877

1. Movements of Objects - The motion of objects in the scene is the most common cause for image blurring. The motion of objects can be classified into three categories: motion of the camera and a static scene, motion of objects with a static camera, and finally the simultaneous motion of both camera and objects in the scene.
2. Movement of the Shutter - Film is exposed in a camera by the movement of the shutter across the film plane. The finite opening and closing time of the shutter, the direction of movement of the shutter as well as changes in the shape of the aperture caused by the movement of the shutter may all modify the appearance of motion blur in the image [13]. In this paper we will not be concerned with modeling the blur arising solely from the functioning of the camera shutter.

The problem of characterizing the degradation caused by an optical system has been the topic of extensive research in image processing [1]. The removal of camera degradation to recover the original image based on some a priori knowledge of the degradation phenomenon is called *image restoration.* In synthesizing motion blur the problem is almost inversed, that is, the objective is to generate an appropriate degradation function given an idealized description of the scene. Although one can draw upon the techniques developed for estimating the optical system-transfer function from a degraded image, the synthesis of an optical system-transfer function from a scene description must take into account the individual motion of objects in the scene, the camera path, the occlusion relationships that may vary between the objects during the exposure time, and any optical effects included as part of the camera model.

The generation of motion blur in computer-synthesized images, as described in this paper, consists of two stages: 1) a hidden-surface program generates intensity sample points of an instantaneous image identifying points which are in motion and giving the image path of the projected motion; and 2) a post-processor which blurs the moving points by convolving them with the optical system-transfer functions derived from the image path and merges them with the stationary points into a final raster image.

A ray-tracing program with a recursive shader [15] generates image point samples, keeping intensity contributions due to surface reflections, transparencies and shadows separate. This allows moving objects reflected in mirrors, transmitted through transparent surfaces, and the shadows of such objects to be blurred. For proper merger of moving objects with stationary objects, intensity samples of the stationary surfaces, hiding or hidden by the moving surfaces, are also computed.

The sample points which contain intensity reflected from moving objects are convolved with an optical system-transfer function, derived from the path and velocity of the motion, and the exposure time. The blurred moving objects and the stationary objects are then merged in a time-and-depth buffer into the final image. In this buffer the visibility of a surface point is determined by its depth, and its intensity is modified by the amount of exposure time it remains visible. A hidden-surface program which processes projected surfaces in a back-to-front order [5] can directly convolve each moving object with its optical system-transfer function as it is stored into the output image.

2.0 Image Formation Model

The camera model which underlies the image-formation process, as modeled here, consists of two stages. First, a 3D scene is projected by a geometric transformation into a 2D *image-irradiance plane.* The image-irradiance plane is then further transformed by the optical system-transfer function, also called a *point-spread function* (PSF), into an actual raster image called the *image-output plane.* The image-output plane simulates a film by acting as a medium for accumulating the radiant energy of objects during the exposure time.

The 3D scene is defined in a homogeneous coordinate system $O(x,y,z,w)$ and contains a set of 3D objects represented by $e_i(x,y,z,w)$, $i=1,2,--,n$ as shown in Figure 1. This representation contains both geometrical and optical properties of the objects. This is referred to as the *object-space* coordinate system. A geometrical transformation function $q(x',y';e_i(x,y,z,w))$ transforms object descriptions from $O(x,y,z,w)$ to $O'(x',y')$ *(image-irradiance plane)* eliminating hidden surfaces of objects and generating the radiant intensity for each visible surface point:

$$f(x',y') = q(x',y';e(x,y,z,w)) \qquad (2\text{-}1)$$

A discrete formulation of the image-irradiance function is

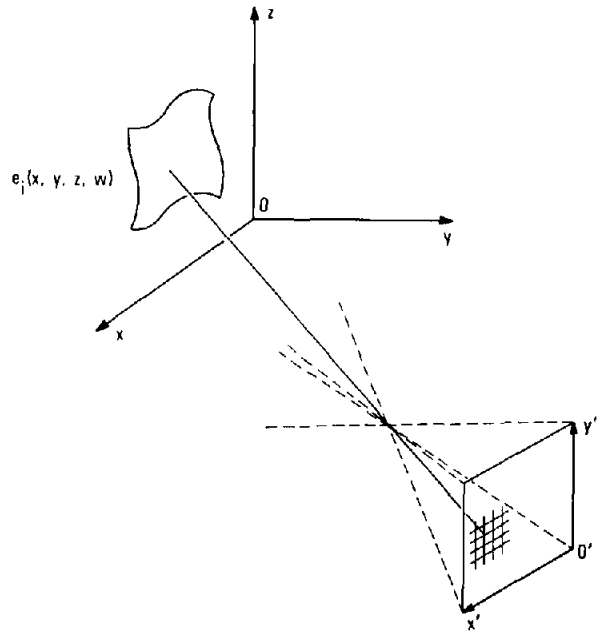

Figure 1 Projection of 3D scene in object space $O(x,y,z,w)$ into image-irradiance plane $O'(x',y')$

equivalent to uniformly sampling the function $f(x',y')$ using a *comb* function (Figure 2) such that

$$f(i\Delta x',j\Delta y') = \sum_{i=0}^{M}\sum_{j=0}^{N} \delta(i\Delta x',j\Delta y')\, f(x',y') \tag{2-2}$$

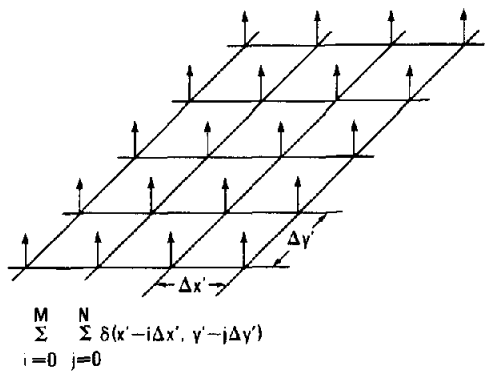

Figure 2 2D comb function of samples of the image-irradiance function in $O'(x',y')$

where $\Delta x'$ and $\Delta y'$ are the sampling intervals in x' and y' directions, respectively. We will assume that the sampling rate is adequate so that we can reconstruct $f(x',y')$ from $f(i\Delta x',j\Delta y')$ by using a suitable interpolating function.

The transformation from the image-irradiance plane $O'(x',y')$ to the image-output plane $O''(x'',y'')$ *(raster image)* incorporates the degradation of the optical system and simulates the imaging medium. We denote this transformation as $h(x'',y''; x',y',f(x',y'))$, and thus we can express the raster image

$$g(x'',y'') = h(x'',y''; x',y',f(x',y')). \tag{2-3}$$

In order to quantify the transformation $h(x'',y'';x',y',f(x',y'))$ we will assume the following properties:

1. The radiant intensity distribution in both the image-irradiance plane and the image-output plane is either positive or zero. This implies that the image-irradiance function (which is a measure of this energy distribution), and any transformations on the image-irradiance function may either conserve the energy or distribute it differently. Thus
$$f(x',y') \geq 0, \text{ and } g(x'',y'') \geq 0. \tag{2-4}$$
2. The radiant intensity distribution is additive in both the image-irradiance plane and the image-output plane. This superposition property implies that given two points $f_1(x',y')$ and $f_2(x',y')$ and their corresponding mapping $g_1(x'',y'')$ and $g_2(x'',y'')$ then
$$f_1(x',y') + f_2(x',y') = g_1(x'',y'') + g_2(x'',y''). \tag{2-5}$$

Based on these two assumptions we may write the transformation from the image-irradiance plane $O'(x',y')$ to the output-image plane $O''(x'',y'')$ in the spatial domain by:

$$g(x'',y'') = \int_{-\infty}^{\infty}\int_{-\infty}^{\infty} h(x'',y'';x',y',f(x',y'))\, dx'\, dy' \tag{2-6}$$

where $h(x'',y''; x',y',f(x',y'))$ is the optical system-transfer function (PSF) describing the energy distribution between points in the image-irradiance plane O' and the output-image plane O''. This is the most general form for describing the image-formation process.

A number of simplifications can be made to the generalized image formation equation (2-6) described above. If the additive components in the image-irradiance plane relate to the additive components in the image-output plane then the system is said to be linear in which case equation (2-6) can be written in the more familiar form of

$$g(x'',y'') = \int_{-\infty}^{\infty}\int_{-\infty}^{\infty} h(x'',y'';x',y')\, f(x',y')\, dx'\, dy' \tag{2-7}$$

The description of the optical system-transfer function in terms of the all four coordinate variables (x'',y'',x',y') reflects space-variance of the transfer function, that is, the transfer function is allowed to vary with position in both the object space and image space. We define such a transfer function as a space-variant PSF (SVPSF). If we restrict the transfer function to be independent of position, that is, the PSF applies uniformly to all points in the object and image space then it is defined as space-invariant (SIPSF) which can be expressed as

$$h(x'',y'';x',y') = h(x''-x',y''-y'). \tag{2-8}$$

In the space-invariant PSF case, the transformation from the image-irradiance plane O' to the image- output plane O'' can be expressed with the convolution integral:

$$g(x'',y'') = \int_{-\infty}^{\infty}\int_{-\infty}^{\infty} h(x''-x',y''-y')\, f(x',y')\, dx'\, dy'. \tag{2-9}$$

We often denote the convolution operation in the spatial domain by the symbol * so that we may equivalently write equation (2-9) as $g(x'',y'') = h(x'',y'')*f(x',y')$. Finally in the discrete formulation $g(x'',y'')$ can be represented by the convolution summation

$$g(i\Delta x'',j\Delta y'') = \sum_{i=0}^{M}\sum_{j=0}^{N} h(i\Delta x''-i\Delta x',j\Delta y''-j\Delta y')\, f(i\Delta x',j\Delta y') \tag{2-10}$$

The equivalent operation in the frequency domain can be written as the product of the fourier transforms of the image-irradiance plane and the PSF:

$$G(u,v) = H(u,v)\, F(u,v). \tag{2-11}$$

For incoherent image formation systems, such as the ones we are trying to model, we only need to consider the squared magnitude of the PSF [4] in the convolution equations described above. The reason for this assumption is that the intensity (radiant energy) is dependent only on the amplitude and not the phase of a electro-magnetic field distribution.

In many cases it is desirable to simplify the computation of convolution by factoring the 2D PSF into two 1D PSFs. This property is called the separability property of

the PSF and can be expressed as follows for the space-invariant case as:

$$h(x'-x'',y'-y'') = h_1(x'-x'')\ h_2(y'-y''). \quad (2\text{-}12)$$

This implies that for an orthogonal coordinate space, the horizontal and vertical transformations can be performed sequentially and independently of each other.

In many instances modeling the camera effects may results in several PSFs cascaded together so that the overall transfer function achieves the desired effect. Given two PSFs $h_1(x'',y'';x',y')$ and $h_2(x'',y'';x',y')$ the overall transfer function $h_{12}(x'',y'';x',y')$ can be expressed as the convolution of the individual transfer functions $h_1(x'',y'';x',y')*h_2(x'',y'';x',y')$. Alternately, in the frequency domain this can be viewed as the product of the two individual transfer functions.

In summary the image formation model can be described by a two stage process as shown in Figure 3. The first is a geometrical transformation which projects the object space onto an image-irradiance plane resolving the hidden surfaces and calculating the radiant intensity for each discrete visible point. We call this process the scene imaging system. An optical system-transfer function (PSF) is then used to transform the image-irradiance plane to the image-output plane. The PSF describes the relationship of the energy distributions between the image-irradiance plane and image-output planes incorporating the effects of the lens, aperture, and shutter. The output-image plane thus acts as an integrating medium accumulating the total radiant energy during the exposure time of the camera.

3.0 Effects of Object Motion and Camera Shutter

3.1 Point-Spread Function of Object Motion

The problem of blurring the output image function $g(x'',y'')$ due to object motion during the exposure time [1,11,12,13] is described in this section. Let the path of the object motion be described in the 3D object coordinate system $O(x,y,z,w)$ as a parametric function of time:

$$\mathbf{r}(t) = \left[\ x(t)\ y(t)\ z(t)\ w(t)\ \right], \quad (3\text{-}1)$$

which is projected into the 2D object coordinate system $O'(x',y')$ as:

$$\mathbf{r}'(t) = \left[\ x'(t)\ y'(t)\ \right] \quad (3\text{-}2)$$

by the geometrical transformation $q(x',y';x,y,z,w)$ as in equation (2-1):

$$\mathbf{r}'(t) = q(x',y';\mathbf{r}(t)). \quad (3\text{-}3)$$

We assume that all the projected points in $f(x',y')$ of an object are moving along a single projected path $\mathbf{r}'(t)$, that is, $\mathbf{r}(t)$ is projected into a space-invariant $\mathbf{r}'(t)$ in $O'(x',y')$. By this we mean that the blurring is applied uniformly to all points along the projected path of motion.

Suppose that the motion of the object can be stopped at some instant t, and this instantaneous image can be expressed as $g(x'',y'',t)$. Then the recorded image-output function $g(x'',y'')$ during the fixed exposure time interval $[0,T]$ is:

$$g(x'',y'') = \int_0^T g(x'',y'',t)\ dt. \quad (3\text{-}4)$$

This integration is physically performed by the film or other recording medium. It can be described as the summation at image output point (x'',y'') of the intensities of all object points that are mapped onto this image point during the exposure interval. Assuming that energy is conserved by the imaging system at any instant during the exposure, energy radiated by an area element $dx'\ dy'$ of $O'(x',y')$ and collected by an area element $dx''\ dy''$ of $O(x'',y'')$ is described by:

$$g(x'',y'',t)\ dx''\ dy'' = f(x',y')\ dx'\ dy' \quad (3\text{-}5)$$

at instant t. Substituting the path description (3-2) into (3-5) and combining it with (3-4) we obtain the recorded image function:

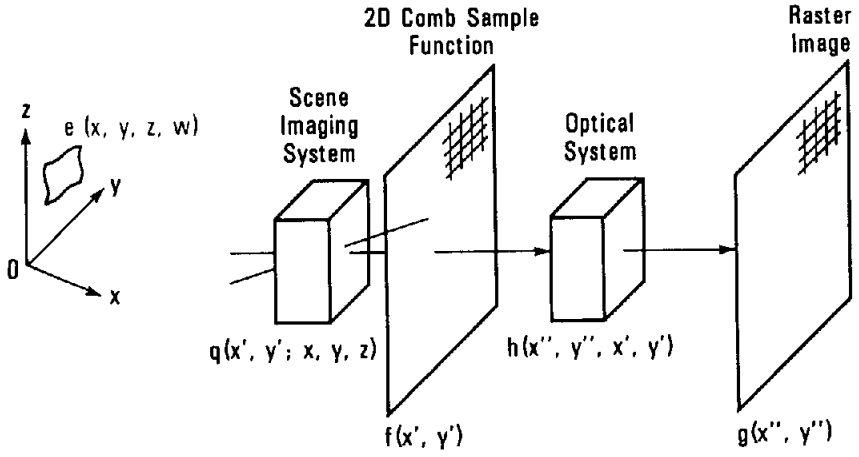

Figure 3 Image-formation system model

$$g(x'',y'') = \int_0^T f(x'(t),y'(t))\ dt. \qquad (3\text{-}6)$$

Given a description of the object motion $\mathbf{r}'(t)$ (3-2) we convert the time integral of the moving object (3-6) into a positional integral over an equivalent stationary object. The elemental length ds of path $\mathbf{r}'(t)$ is given by:

$$ds = \left[\left(\frac{dx'(t)}{dt}\right)^2 + \left(\frac{dy'(t)}{dt}\right)^2\right]^{1/2} dt. \qquad (3\text{-}7)$$

Therefore the time integral in equation (3-6) can be changed into line integral of the form:

$$g(x'',y'') = \int_{\mathbf{r}'(0)}^{\mathbf{r}'(T)} \frac{f(x',y')\ ds}{\left[\left(\frac{dx'(t)}{dt}\right)^2 + \left(\frac{dy'(t)}{dt}\right)^2\right]^{1/2}} \qquad (3\text{-}8)$$

which is a general expression for motion degradation with the linear space-invariant model of equation (2-9). The SIPSF can be identified in equation (3-8) as:

$$h(x'',y'';x',y') = \left[\left(\frac{dx'(t)}{dt}\right)^2 + \left(\frac{dy'(t)}{dt}\right)^2\right]^{-1/2}_{\substack{t = x'^{-1}(\mathbf{r}_x) \\ t = y'^{-1}(\mathbf{r}_y)}} \qquad (3\text{-}9)$$

where $x'(t)$ and $y'(t)$ are valid over the path of the object motion, that is,

$$x'(0) \leqslant x'(t) \leqslant x'(T)$$
$$y'(0) \leqslant y'(t) \leqslant y'(T)$$

and $h(x'',y'';x',y') = 0$ elsewhere. The amplitude of the response is, therefore, inversely proportional to the velocity of the motion of an object point, i.e., as the object moves faster its image spreads over a greater image area with reduced intensity. Since the derived $h(x'',y'';x',y')$ is space invariant, the convolution in equation (2-10) with this PSF can be performed either in the spatial or the frequency domain.

Consider a simple example where $\mathbf{r}'(t) = x_0(t)$ describes planar motion of the object in the x-direction. Using (3-6) we may write

$$g(x'',y'') = \int_0^T f(x'-x_0(t),\ y')\ dt, \qquad (3\text{-}10)$$

and from the frequency-domain relationship in (2-11):

$$G(u,v) = \int_{-\infty}^{\infty}\int_{-\infty}^{\infty}\left[\int_0^T f(x'-x_0(t),\ y')dt\right] e^{-j2\pi(ux'+vy')}dx'dy'. \qquad (3\text{-}11)$$

By reversing the order of integration and using the shifting property of Fourier transforms $G(u,v)$ can be expressed as

$$G(u,v) = F(u,v)\int_0^T e^{-j2\pi(ux_0(t))}\ dt \qquad (3\text{-}12)$$

Let $x_0(t) = \frac{at}{T}$, and $0 \leqslant t \leqslant T$. Using (2-11) we identify

$$H(u) = \int_0^T e^{-j2\pi x_0(t)}\ dt. \qquad (3\text{-}13)$$

Substituting for $x_0(t)$, we obtain

$$H(u) = \int_0^T e^{-j2\pi\frac{uat}{T}}\ dt = \frac{T}{\pi ua}\sin(\pi ua)\ e^{-j\pi ua} \qquad (3\text{-}14)$$

Alternatively, one may directly obtain $h(x'')$ by substituting into (3-9)

$$h(x'') = \frac{T}{a}, \text{ where } 0 \leqslant x'' \leqslant a \qquad (3\text{-}15)$$

It is easy to verify that (3-15) is indeed the inverse Fourier transform of (3-14). An example of uniform motion blur is shown in Figure 4. This simulates the motion of a camera viewing a static scene. Figure 4(a) shows the original natural image; the Fourier spectrum of this image is shown in Figure 4(b). This FFT was multiplied by the frequency-domain uniform blur function $x_0(t)$. The convolved image is shown in Figure 4(c) and the inverse FFT producing the blurred image is shown in Figure 4(d).

In a space-variant system where each point of a moving object may follow a different path $\mathbf{r}'(t)$ it is necessary to compute the path $\mathbf{r}'(t)$ and the PSF $h(x'',y'';x',y')$ of the path separately for each moving point in $f(x',y')$. Sawchuk [12] has shown that for a large class of motions it is possible to change a space-variant system by a geometrical coordinate transformation into a space-invariant system.

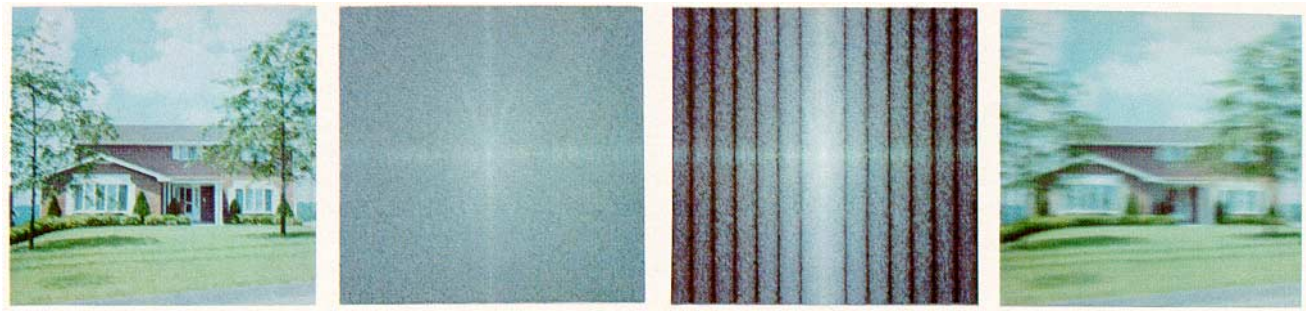

(a) (b) (c) (d)

Figure 4 Uniform motion-blur with frequency-domain computations: (a) original image, (b) FFT of original image, (c) FFT convolved with PSF, (d) blurred image

3.2 Point-Spread Function of Camera Shutter

In the previous section we obtained a PSF due to object motion assuming instantaneous shutter opening at time $t = 0$ and closing at time $t = T$. Most actual shutters, however, are mechanical devices which vary the shape of the aperture during their opening and closing times and therefore further modify the system PSF. Shack [13] derived the shutter PSF's for the two most common types of shutter.

The *focal-plane shutter* is a narrow slit in a curtain which moves across the film frame, slightly in front of the film plane, usually in the x'' (horizontal) direction. The aperture remains open for the duration of the exposure. The exposure is controlled by the speed of the curtain motion and the width of the slit. The PSF for this shutter type is in the frequency domain [13]:

$$H(u,v) = \begin{cases} 1 - \dfrac{|u|}{d} & 0 < |u| < d \\ 0 & |u| > d \end{cases} \qquad (3\text{-}16)$$

where d is the ratio of the width of the curtain slit moving in the x'' direction and the radius of the aperture opening.

The *between-the-lens shutter* consists of a usually circular or star-shaped opening made of several blades, placed between lens elements, and similar in construction to the aperture diaphragm. The size of the shutter diaphragm increases as the shutter opens and decreases as the shutter closes. The aperture diaphragm of the lens remains open all the time. The PSF of this shutter type is substantially more complicated [13] than (3-10), and can be best approximated by a PSF of a circular aperture [6,7] whose radius varies with time.

The PSF's due to motion of objects and camera may be cascaded with the PSF due to the shutter into a single system-transfer function [Figure 5].

4.0 Synthetic Image Generation

4.1 Hidden-Surface Elimination

A ray-tracing hidden-surface processor is used to compute the intensity point samples in $O'(x',y')$ from a description of a 3D scene and the camera geometry. The processor uses Whitted's recursive-illumination model [15] to compute intensity-point samples with the following shading equation:

$$f(i\Delta x', j\Delta y') = I_a + I_d + I_s + I_r + I_t \qquad (4\text{-}1)$$

where

I_a = the ambient light intensity,
I_d = the the diffuse reflection,
I_s = the specular reflection,
I_r = the reflected light intensity, and
I_t = the transmitted light intensity.

This equation can be recursively redefined for I_r and I_t. The intensity change due to a shadow cast by an opaque object is:

$$I_{shadow} = -I_d - I_s \qquad (4\text{-}2)$$

The hidden-surface program generates a raster image with a pin-hole camera model, and optionally the separate image intensity samples $f(i\Delta x', j\Delta y')$ [6,7]. Each sample consists of the following information obtained from a node of the shading tree at $O'(i\Delta x', j\Delta y')$:

1. the type of intensity information contained in the node: opaque, reflected, transmitted, hidden, or shadow.
2. the (i,j) coordinates of the sampled point,
3. the red, green, and blue intensity values, I_{red}, I_{green}, and I_{blue}, contributed by the measured object point,
4. the z' depth (along the camera's optical axis) of the measured object point (not used for shadows), and
5. the object identification number of the measured point (or object identification number of object casting shadow).

The list of samples of an image frame is then passed to a motion-blur processor together with a list of motion paths of the individual objects, time of the frame exposure t_{frame}, and the exposure duration T_{frame}. In an actual animation system, this information would be provided by an animation processor [2,9,14] which controls the motions of the objects and the camera.

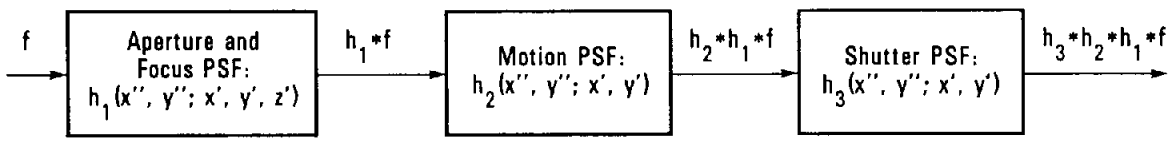

Figure 5 Cascaded system of point-spread functions

4.2 Addition of Motion Blur

Motion blur is generated by a processor shown in the block diagram in Figure 6. This processor separates sample points of a moving object with the same path $\mathbf{r}'(t)$ into a raster image **f**. The motion blur PSF $h(x'',y'';x'y')$ (equation 3-9) is computed from the object path $\mathbf{r}'(t)$, the exposure time t_{frame}, and the exposure length T_{frame} as a raster image **h**. The images **f** and **h** are then convolved into a blurred image **f*h**. This convolution can be performed either directly in the spatial domain, or optionally images **f** and **h** can be converted by FFT into **F** and **H**, respectively, in the frequency domain, multiplied into **F·H**, and then converted back into **f*h** by an inverse FFT. Finally, all blurred images of the moving objects are merged with the image of the stationary objects into the output raster image.

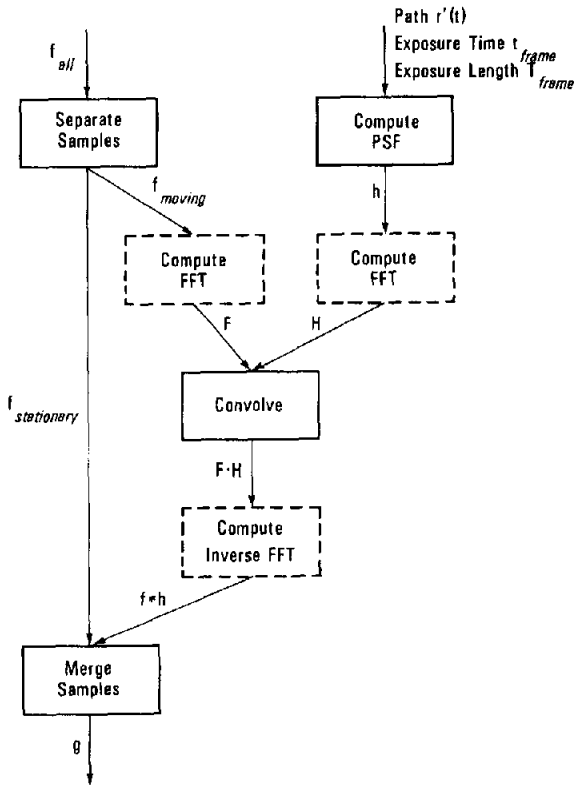

Figure 6 Block diagram of the motion-blur processor

To merge the stationary image with the blurred images of the moving objects, we need to compute in each blurred image the fraction of the exposure length T_{frame} that the moving object overlaps each pixel. From this information we can also determine the amount of time T_{frame} that each pixel in the stationary image is visible. This is accomplished by adding a fourth band (to the red, green and blue intensity bands) to each image **f**. This band contains the exposure length T_{frame} in every pixel that the instantaneous image of the moving object overlaps and 0 elsewhere. This "time" band is convolved with the PSF **h** exactly as the three image intensity bands. In image **f*h** this band, therefore, contains the fraction of time T_{frame} that the moving object overlaps each pixel. The hidden-surface processor also generates intensity samples of stationary objects hiding or hidden by the moving objects. (Intersections with hidden-surfaces are otherwise used by this program for processing solid objects [10].) The stationary image is an image of the scene without the moving objects, rather than an image with "black holes" in places where the moving objects are missing. The blurred images of the moving objects and the image of the stationary objects are merged in a time-and-depth buffer. In this buffer the visibility of each pixel in the images being merged is determined by its depth, and its intensity by the length of time it remains visible. If a stationary surface is hiding a moving surface, the time exposure and therefore the intensity of the moving surface are reduced to 0. Otherwise, if one or more moving surfaces are hiding a stationary surface, the intensity of the stationary surface is reduced by the amount of time it is invisible which is determined from the exposure time value computed in each blurred image **f*h**. If the sum of the computed exposure times of the moving surfaces exceeds T_{frame} at a given pixel, then the intensity of the blurred moving surfaces is also appropriately reduced, and the stationary surface becomes, of course, completely invisible.

5.0 Results

The image sample functions are generated from a 3D scene description by a ray-tracing program previously described in [6,7]. Moving objects are assigned paths from which the motion-blur PSF's are computed. The motion-blur generation, as described in the previous section (Figure 6), has been implemented in both the spatial and frequency domains.

The first example (Figure 7) illustrates the use of multiple PSFs to describe the motions of several objects in a scene. Figure 7(a) shows an instantaneous image of a magnet and ten metallic balls suspended in air. In Figure 7(b) the balls accelerate along their individual paths toward the magnet during an exposure time T. In Figure 7(c) the exposure time has been doubled to $2T$ with a corresponding increase in the motion blur. In Figure 7(d) the PSF's of the balls have been modified to simulate a multiple exposure. During the total exposure time $2T$ the shutter was opened five times at $0.4T$ intervals, and each time remained open for $0.2T$. Note in the last three images that the intensity of the moving objects diminishes as the velocity of the objects increases.

In the second example motion blur is applied to an image containing reflections and refractions of moving objects. The instantaneous image (Figure 8(a)) consists of a cube with an image of a mandrill mapped on its six sides and three transparent spheres. These four objects are reflected in a planar mirror. The finite-exposure image

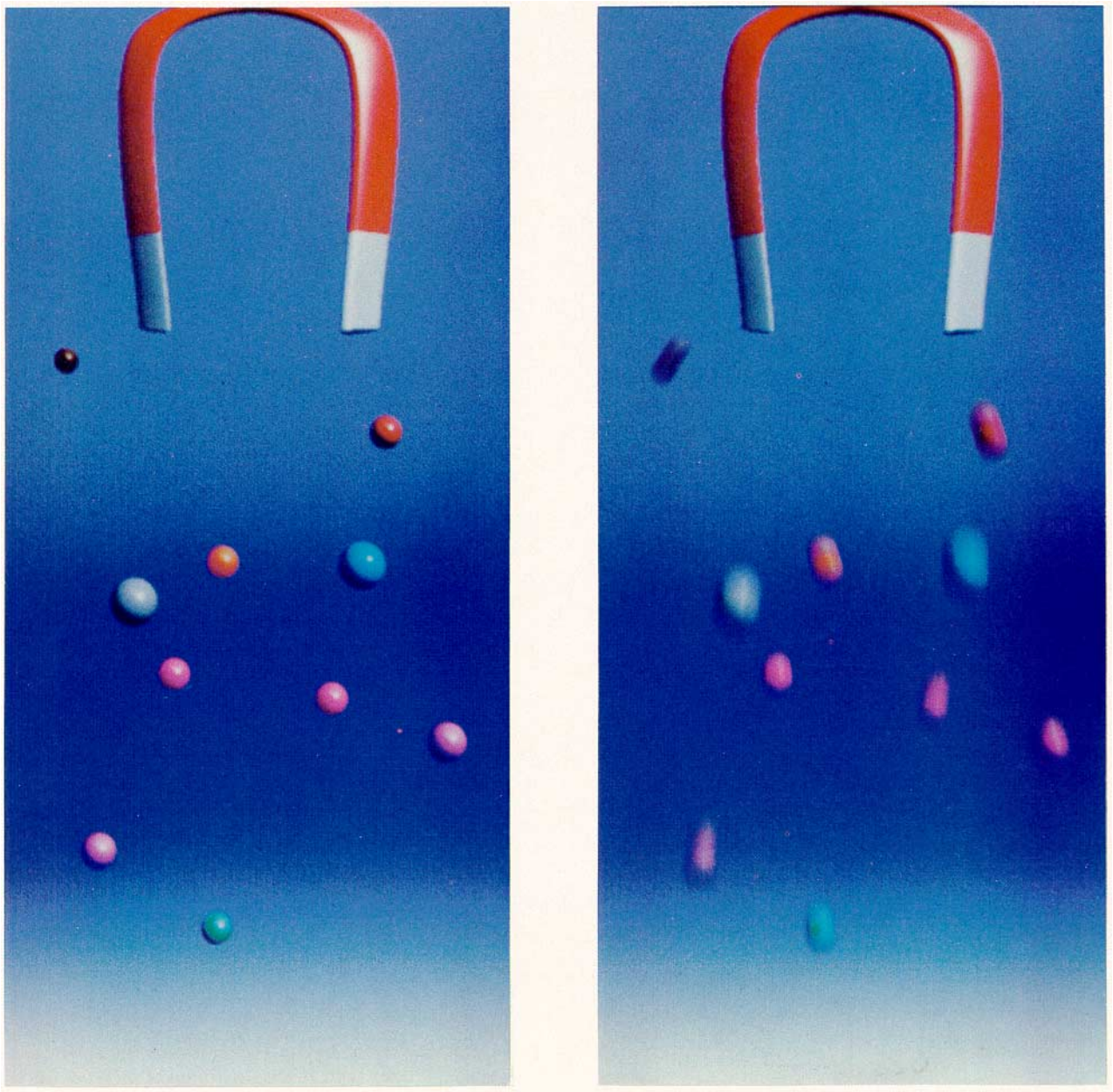

Figure 7 Magnet attracting metallic balls: (a) instantaneous exposure, (b) finite-time exposure

(Figure 8(b)) shows motion blur of the cube and the three spheres as well as their reflections in the mirror. This is accomplished by convolving the motion blur PSF's of an object with all of its image samples (including reflections and refractions) generated by the hidden-surface program.

6.0 Conclusions

This paper has expanded upon a previously-described model of a camera's optical system [6,7] to include motion blur, that is, the ability to integrate image intensity due to moving objects during the time that a camera shutter remains open.

The camera model has been described in terms of a generalized image-formation system. This has allowed us to express the motion of objects by a set of optical system-transfer functions which are applied to the points in the image exhibiting the same motion, effectively simulating the camera shutter. In addition, this model allows us to cascade several transfer functions where each transfer function contributes one aspect of the overall camera

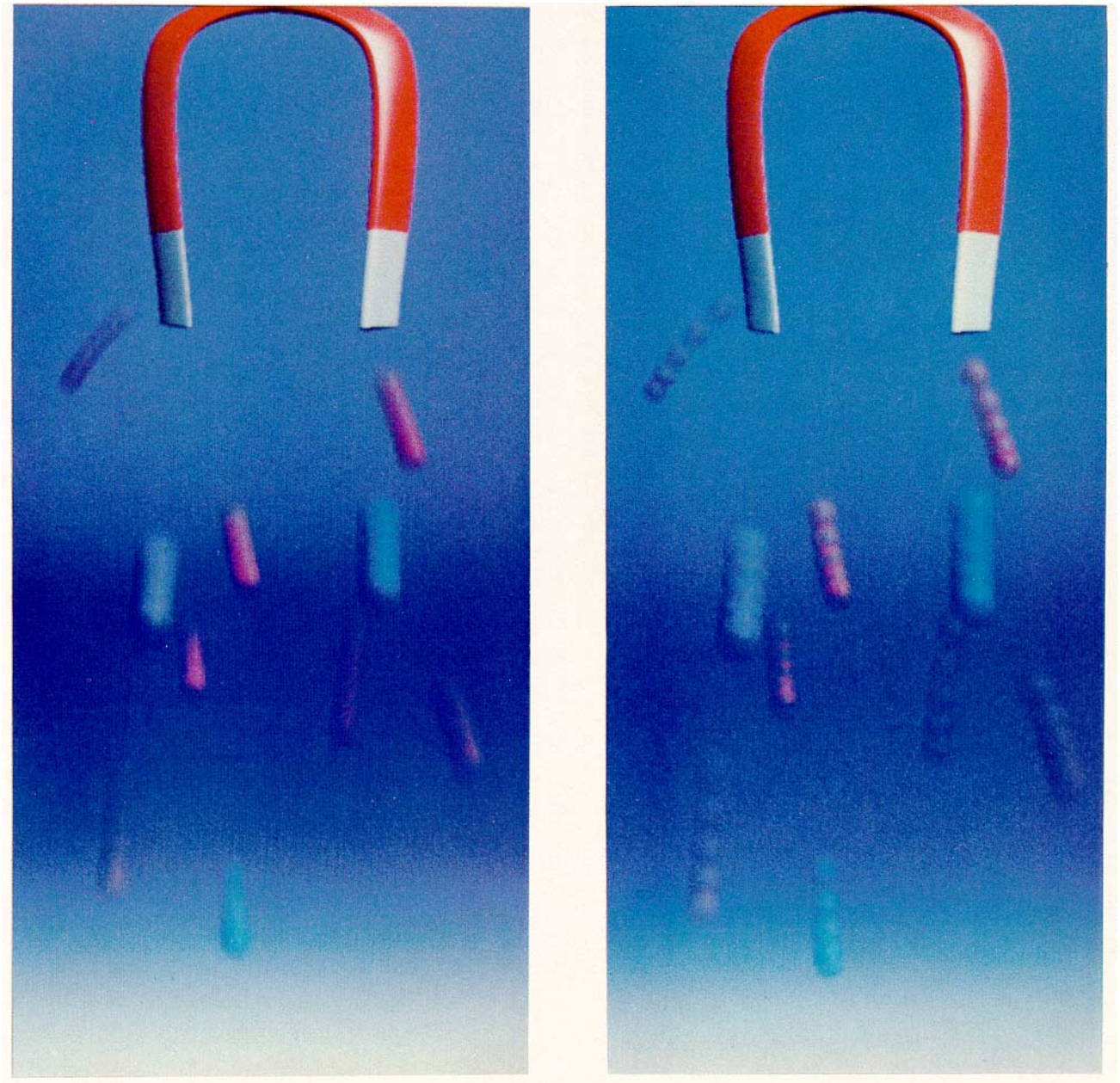

(c) (d)

Figure 7 Magnet attracting metallic balls: (c) extended time-exposure, (d) multiple exposure

model.

The implementation of this procedure has been attempted in both the spatial and frequency domains. A general expression for modeling the PSF of an arbitrary motion has been derived. This model has been applied to a 3D scene with multiple objects, each with its own path and velocity description, to generate images simulating motion blur. Examples of uniform blur due to camera motion and blur of reflected and refracted objects have been also presented. The modeling of motion blur in the most general case can become complicated due to object occlusions that may occur during the exposure time.

In this paper we have considered primarily the camera effects due to the lens, aperture, and shutter and their use in image synthesis. Future enhancements could be in the area of modeling special-effect filters (star, diffraction), the lens transfer function (optical aberrations) and the noise introduced by the optical system and the imaging medium.

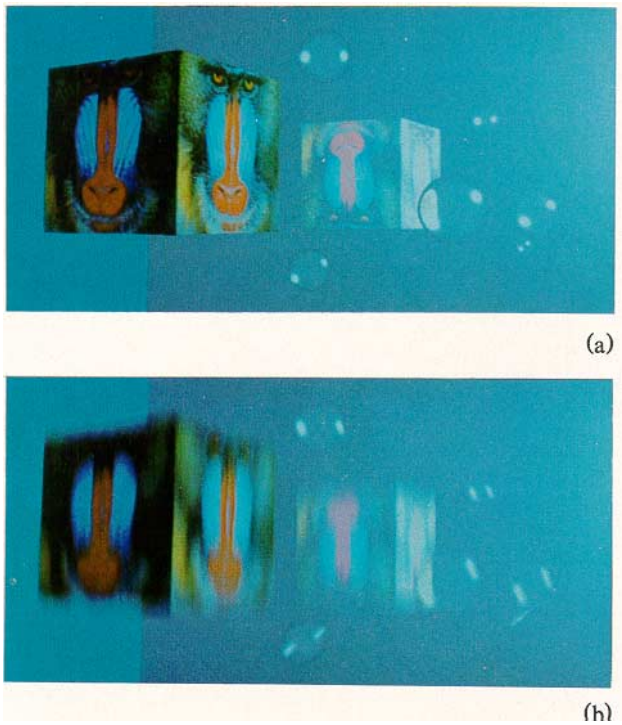

Figure 8 Mandrill cube and transparent spheres reflected in a mirror: (a) instantaneous image, (b) finite-time exposure image

7.0 Glossary

Symbol	*Description*
$e(x,y,z,w)$	surface representation in $O(x,y,z,w)$
$f(x',y')$	image-irradiance function in $O'(x',y')$
$f(x',y',t)$	image-irradiance function in $O'(x',y')$ at time t
$F(u,v)$	image-irradiance function in frequency domain
$g(x'',y'')$	image-output function in $O''(x'',y'')$
$g(x'',y'',t)$	image-output function in $O''(x'',y'')$ at time t
$G(u,v)$	image-output function in frequency domain
$h(x'',y'';x',y')$	optical transfer function from $O'(x',y')$ to $O''(x'',y'')$
$H(u,v)$	transfer function $h(x'',y'';x',y')$ in frequency domain
$O(x,y,z,w)$	3D object coordinate system
$O'(x',y')$	2D image-irradiance coordinate system
$O''(x'',y'')$	2D image-output (raster) coordinate system
$q(x',y';x,y,z,w)$	geometrical transformation function from $O(x,y,z,w)$ to $O'(x',y')$
$\mathbf{r}(t)$	object path in $O(x,y,z,w)$
$\mathbf{r}'(t)$	projection of path $\mathbf{r}(t)$ into $O'(x',y')$
t	time parameter
T	exposure time
$\delta(x',y')$	impulse-response function in $O'(x',y')$
$\Delta x'$	sampling distance of input function $f(x',y')$ in x'
$\Delta x''$	pixel size of output function $g(x'',y'')$ in x''
$\Delta y'$	sampling distance of input function $f(x',y')$ in y'
$\Delta y''$	pixel size of output function $g(x'',y'')$ in y''

Abbreviations

FFT	fast Fourier transform
PSF	point-spread function
SIPSF	space-invariant point-spread function
SSIPSF	separable space-invariant point-spread function
SSVPSF	separable space-variant point-spread function
SVPSF	space-variant point-spread function

8.0 Acknowledgments

The authors would like to thank Henry Moreton of Schlumberger-Doll Research for designing the 3D model of the magnet.

9.0 References

[1] Andrews, H. C. and Hunt, B. R., *Digital Image Restoration*, Prentice Hall Inc., New Jersey, 1977

[2] Blinn, J. F., "Systems Aspects of Computer Image Synthesis and Animation", SIGGRAPH 1982 Tutorial Notes

[3] Dainty, J. C., and Shaw, R., *Image Science*, Academic Press, New York, 1974

[4] Goodman, J. W., *Introduction to Fourier Optics*, McGraw-Hill, Inc., New York, 1968, Chapter 4,5

[5] Newell, M. E., Newell, R. G., and Sancha, T. L., "A New Approach to the Shaded Picture Problem", *Proceedings of the ACM National Conference*, 1972

[6] Potmesil, M. and Chakravarty, I., "A Lens and Camera Model for Synthetic Image Generation", *ACM Computer Graphics (Proc. SIGGRAPH 1981), 15*, (3), 297-305, August 1981

[7] Potmesil, M. and Chakravarty, I., "Synthetic Image Generation with a Lens and Aperture Camera Model", *ACM Transactions on Graphics, 1*, (2), 85-108, April 1982

[8] Pratt, W. K., *Digital Image Processing*, Wiley-Interscience, New York, 1978

[9] Reynolds, C. W., "Computer Animation with Scripts and Actors", *ACM Computer Graphics (Proc. SIGGRAPH 1982), 16*, (3), 289-296, July 1982

[10] Roth, S., "Ray Casting for Modeling Solids", *Computer Graphics and Image Processing, 18*, (1), 109-144, January 1982

[11] Sawchuk, A. A., "Space-Variant Image Motion Degradations and Restorations", *Proc. IEEE*, *60*, (7), 854-861, July 1972

[12] Sawchuk, A. A., "Space-Variant Image Restoration by Coordinate Transformation", *JOSA*, *64*, (2), 138-144, February 1974

[13] Shack, R. V., "The Influence of Image Motion and Shutter Operation on the Photographic Transfer Function", *Applied Optics*, *3*, (10), 1171-1181, October 1964

[14] Shelley, K. L., and Greenberg, D. P., "Path Specification and Path Coherence", *ACM Computer Graphics (Proc. SIGGRAPH 1982)*, *16*, (3), 157-166, July 1982

[15] Whitted, T., "An Improved Illumination Model for Shaded Display", *Comm. ACM*, 3, (6), June 1980, 343-349